HARMONIC CONTENTS OF AND DETAILED STUDY ON A HIGH-GAIN HARMONIC GENERATION FREE ELECTRON LASER*

Juhao Wu†
SLAC, Stanford University, Stanford, CA 94309

Abstract

In this paper, we calculate the third harmonic of a High Gain Harmonic Generation (HGHG) Free Electron Laser (FEL) at saturation. In the HGHG FEL scheme, there is an external dispersion section, which provides an efficient microbunching. Study on the emittance effect in such an external dispersion section suggests a new optimization for the HGHG FEL. We finally discuss how to reduce the incoherent undulator radiation which is a noise with respect to the seed laser.

INTRODUCTION

High-Gain Harmonic Generation (HGHG) Free-Electron Laser [1] is perceived as a candidate for a coherent light source in the Deep UV to X-ray regime [2, 3]. So far, our main interest is on the fundamental radiation [2]. However, at the end of the amplifier, the HGHG FEL is in deep saturation regime, hence harmonic contents are significant. These harmonic contents [4, 5] are the natural extension to shorter wavelengths. We hence upgrade the TDA simulation code [6] to calculate the harmonics.

To enhance the microbunching process, in the HGHG scheme, an external dispersion section is adopted. Such a dispersion section enhances microbunching more efficiently than the undulator does. Besides this, emittance effect is less stringent in the external dispersion section than in the undulator. This then provides a new optimization scheme.

When it passes through the undulator together with the seed laser, the electron beam will produce undulator radiation, which is a noise with respect to the seed laser. We suggest an approach to reduce such noise effect.

TDA-HARMONICS SIMULATION CODE

Numerical simulation of Self-Amplified Spontaneous Emission (SASE) FEL is normally performed using time-dependent computer codes [7], which require large CPU time and memory. Time-independent simulation code such as TDA [6] relaxes this, though people normally think it will be less accurate. Previous studies proved that TDA is still a very useful code as long as we use it properly [8]. For HGHG FEL, the input seed laser well dominates the shot noise, so TDA is sufficient. We therefore upgraded the TDA code to include harmonics. We test our code against published results [5, 9, 10].

Equations of motion

We keep the same notation as those in TDA. We here present the dynamics equations for a planar undulator. Similar to TDA, TDA-Harmonics (TDA-H) uses the following two equations for the longitudinal motion: one for the Lorentz factor γ and the other for the electron phase $\theta = (k_s + k_w)z - \omega_s\, t$. They are

$$\frac{d\gamma}{dz} = \frac{k_s a_w}{\gamma} \sum_{f=1}^{\infty} f\,\mathrm{Re}\{G_f\}, \tag{1}$$

and

$$\frac{d\,\theta}{d\,z} = k_w - \frac{k_s}{2\gamma^2}\left[1 + a_w^2 + \gamma^2\beta_{\perp 0}^2 - 2a_w \sum_{f=1}^{\infty} \mathrm{Im}\{G_f\}\right]; \tag{2}$$

where,

$$\begin{aligned} G_f \;\equiv\;& (-i)^{f-1}\exp(if\,\theta) \times \left(\frac{i\beta_{x0}\gamma}{\sqrt{2}a_w} K_f^{\perp} a_s^f \exp(i\phi_s^f)\right. \\ &+\; iK_f^{(1)} a_s^f \exp(i\phi_s^f) \\ &+\; \left.\frac{a_w}{\sqrt{2}\gamma k_w} K_f^{(2)} \frac{\partial}{\partial x}(a_s^f \exp(i\phi_s^f))\right). \end{aligned} \tag{3}$$

Here, the radiation field is characterized by the wavenumber $k_s = 2\pi/\lambda_s = \omega_s/c$, the dimensionless vector potential rms value $a_s = eA_s/(mc)$ and the phase ϕ_s. The wiggler field is specified by the wavenumber k_w and vector potential $a_w = eB_w/(mck_w)$. In these equations, $\beta_{\perp 0} = \sqrt{\beta_{x0}^2 + \beta_{y0}^2}$ is the transverse drift speed and β_{x0} and β_{y0} are the smooth motions of the guiding center. In addition, f is the harmonic number, and the K functions are defined the same as Eqs. (34) and (A7) in Ref. [11], i.e.,

$$\begin{aligned} K_f^{(m)}(\xi,\sigma) \;\equiv\;& (-1)^f \sum_{-\infty}^{+\infty} J_n(f\xi) \\ &\times\; [(-1)^m J_{2n+f-m}(f\sigma) - J_{2n+f+m}(f\sigma)] \end{aligned} \tag{4}$$

and

$$K_f^{\perp}(\xi,\sigma) \equiv 2(-1)^f \sum_{-\infty}^{+\infty} J_n(f\xi) J_{2n+f}(f\sigma), \tag{5}$$

*The work was supported by the U.S. Department of Energy under Contract No. DE-AC03-76SF00515.

† jhwu@SlAC.Stanford.EDU

where,

$$\xi \equiv \frac{a_w^2 k_s}{4\gamma^2 k_w}, \tag{6}$$

and

$$\sigma \equiv \sqrt{2} a_w \beta_{x0} k_s/(\gamma k_w). \tag{7}$$

Notice, our a_w, the same as that in TDA is the rms value, while a_w in Ref. [11] is the peak value.

The two dynamic equations (1) and (2) should be compared with Eqs. (1.a) and (1.b) in Ref. [6]. The equations of the transverse motions are not changed formally.

Wave equation

There are f equations, each stands for a harmonic field. They are

$$\begin{aligned}\left[\frac{\partial}{\partial z} \quad + \quad \frac{1}{2ifk_s}\nabla_\perp^2\right] a_s^f \exp(i\phi_s^f) \\ = \quad i^f \frac{eZ_0}{mc^2}\frac{1}{2fk_s}\frac{I}{N}\sum_{j=1}^{N}\delta(y-y_{0j})\frac{a_w}{\gamma_j}\exp(-if\,\theta_j) \\ \times \quad \left\{\frac{\beta_{x0j}\gamma_j}{\sqrt{2}a_w}K_f^{\perp}\delta(x-x_{0j}) + K_f^{(1)}\delta(x-x_{0j})\right. \\ + \quad \frac{iK_f^{(2)}}{2}\left[\delta\left(x-x_{0j}-\frac{a_w}{\sqrt{2}\gamma_j k_w}\right)\right. \\ - \quad \left.\left.\delta\left(x-x_{0j}+\frac{a_w}{\sqrt{2}\gamma_j k_w}\right)\right]\right\}. \end{aligned} \tag{8}$$

The power balance equation could be derived straightforward and it could be used as a self-check for the numerical simulation results.

Initial conditions

We specify the electron distribution function on the 6-dimensional phase space $F(\gamma, \phi, p_x, x, p_y, y)$ at the entrance of the wiggler at $z = 0$. For the initial radiation field, we assume a Gaussian TEM_{00} mode at $z = 0$ for each harmonic as well as for the fundamental radiation as what was done in TDA.

Preliminary results

We compare TDA-H with TDA and other available results. Good agreements are found. Summary is in Table 1, where we compare with the experiments and make prediction for the LCLS project at SLAC as well.

Now, let us study the harmonic content in an x-ray HGHG FEL. In our scheme [2], there is a 33.5 m long amplifier, which is resonant at 1.5 $\mathring{A}$. In the amplifier, the HGHG FEL is in the deep saturation regime, hence substantial harmonic contents are expected. We use TDA-H to calculate the 3rd harmonic content. The result shows that there is about 30 MW radiation at the third harmonic, i.e. at 0.5 $\mathring{A}$. The evolution of the radiation power in the amplifier is illustrated in Fig. 1. Different from the SASE FEL, the electron beam in HGHG FEL is already highly microbunched when it enters the final amplifier. Hence, the harmonic contents have quite large initial power. This is explicitly shown in Fig. 1, though, initially, there is not much growth for the harmonics. Basically the electron beam and the harmonic exchange energy back and forth, but not much net growth in the harmonic power. Later, when the fundamental radiation is exponentially amplified, the bunching at the harmonics is also enhanced substantially. This is the nonlinear region for the harmonics [5].

		TDA-H	TDA	Ref.
LCLS 1.5 Å	Fund.	14 GW	14 GW	8 GW
	3rd	28 MW		15 MW
LCLS 4.5 Å	Fund.	9 GW	9 GW	7 GW
	3rd	35 MW		40 MW
LETUL SASE	Fund.	76 MW	78 MW	70 MW
	3rd	520 kW		600 kW
ATF HGHG	Fund.	33 MW	35 MW	30 MW
	3rd	630 kW		350 kW

Table 1: Comparison of the results from TDA-H with those from TDA[6] and other references. For ATF HGHG experiment, we use Ref. [9]; for the others. we refer to Ref. [5].

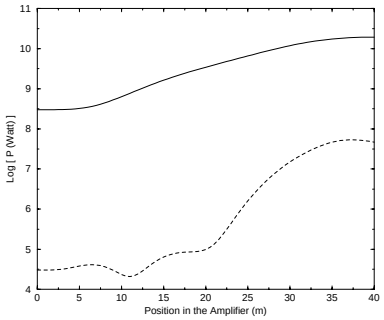

Figure 1: The evolution of the radiation power in the amplifier. The vertical axis stands for the logarithm of the radiation power to the base of 10. The solid line is for the fundamental radiation at 1.5 $\mathring{A}$; and the dashed line for the 3rd harmonic at 0.5 $\mathring{A}$.

EMITTANCE EFFECTS

In the SASE FEL, the microbunching is produced purely in the undulator. The path length difference induced by the energy spread and that by the emittance are both second-order effect. Hence, the emittance is an important effect, which will lead to microbunch diffusion. In the HGHG FEL, there is an external dispersion section, where the path length difference produced by the energy modulation is a first order effect, hence the emittance is not important[12].

We called this the Natural Emittance Effect Reduction (NEER) mechanism.

In an undulator, the effective energy spread due to the emittance is

$$\left.\frac{\sigma_\gamma}{\gamma}\right|_{eff,\epsilon}^{undul} = \frac{k_s\,k_\beta}{2\,k_w}\,\epsilon, \tag{9}$$

where k_β is the betatron wavenumber.

In an idealized dispersion section, the emittance acts like an effective energy spread of

$$\left.\frac{\sigma_\gamma}{\gamma}\right|_{eff,\epsilon}^{disp} = \frac{48\,R^2\,\epsilon}{L_s^2\,\beta} \approx \frac{k_s\,k_\beta\,L_s\,\epsilon}{\gamma\,\left.\frac{d\psi}{d\gamma}\right|_{disp}}, \tag{10}$$

where k_s is the wavenumber in the radiator, and $L_s = 4L_1$ is the total length of the dispersion section, which is assumed to consist of 4 pieces of dipole, each is L_1 long.

The ratio of these two effects is then

$$\eta \equiv \left(\left.\frac{\sigma_\gamma}{\gamma}\right|_{eff,\epsilon}^{disp}\right) \Bigg/ \left(\left.\frac{\sigma_\gamma}{\gamma}\right|_{eff,\epsilon}^{undul}\right) = \frac{2L_s k_w}{\gamma\,\left.\frac{d\psi}{d\gamma}\right|_{disp}}. \tag{11}$$

This ratio is generally small due to the huge γ. A detailed study [13] on our cascading HGHG approach [2] shows that the effective energy spread due to the emittance in the dispersion section is far smaller than that in the undulators. Hence, by reducing the undulator length, the emittance effect is greatly reduced. This NEER mechanism suggests a new operation mode [13], i.e., we could use an electron bunch with a higher current, though an unavoidably higher emittance, in the Harmonic Generation stages.

INCOHERENT/COHERENT SYNCHROTRON RADIATION EFFECT

Saldin *et al.* [14] pointed out that the undulator radiation is the noise with respect to the seed laser. The Noise-To-Signal (NTS) ratio is increased by a factor of N_h^2, where N_h is the harmonic number. Hence, for the cascading HGHG approach [13], the worst problem comes at the first stage. To overcome this, in the modulator of the first stage, we increase the input seed power to 1 GW. Then the final NTS ratio is about 14% in the 1.5 Å HGHG FEL. The first sideband locates at $1/(2\,N_h\,N_u)$ [13], where N_u is the number of undulator period. Hence, as long as this sideband is outside the signal bandwidth, it would not be a concern. In the radiator, together with the HGHG FEL, there will be a SASE FEL. In order to reduce the SASE FEL, we increase the energy modulation $\Delta\gamma$ produced in the modulator, and reduce the dispersion strength $\frac{d\psi}{d\gamma}$ in the dispersion section accordingly to keep $\Delta\gamma\,\frac{d\psi}{d\gamma}$ constant. Recall that the bunching factor

$$b_n \equiv \exp\left[-\frac{1}{2}\,\sigma_\gamma^2\,\left(\frac{d\psi}{d\gamma}\right)^2\right]\,J_n\left[\Delta\gamma\left(\frac{d\psi}{d\gamma}\right)\right]. \tag{12}$$

Hence, by doing so, b_n is increased! Now recall that the start-up coherent emission (CE) power $P^{Coh} \propto |b_n|^2$ [13]. Hence the start-up CE power is in fact increased! However, since the energy modulation is an effective energy spread, the power e-folding length increases to be $L_{Gr} = 0.9$ m, while $L_{Gr} = 0.6$ m for the case without energy modulation [2]. Because of the larger energy spread, the saturation power is reduced. At about $L_{Rad.} = 4$ m, the system reached saturation. In such a radiator the SASE FEL is only about 2 kW. Recall that the HGHG FEL has a power of 10 GW, and now $N_h = 450/1.5 = 300$. The final NTS ratio is about 2%. The contribution from the other undulators is smaller because N_h is reduced along the device. Hence, the undulator radiation is not serious.

The dispersion section between two adjacent undulators is essentially a bunch-compression chicane. As an estimate, we assume an ideal dispersion section, i.e., a three-dipole chicane with no drift space among the dipoles, so that the length of the first and third magnets both to be L_1, the middle magnet length to be $2L_1$. The momentum compaction is $R_{56} = 4L_1\left(\frac{1}{\cos\psi} - \frac{\psi}{\sin\psi}\right)$, where ψ is the bending angle. Now we hope to get a path difference of $\lambda_r/4$ for a relative energy modulation of $\Delta\delta$, i.e. $\lambda_r/4 = R_{56}\Delta\delta$. If we assume the magnetic field to be $B = 0.5$ Tesla, and $L_1 = 8$ cm, then the bending angle is only $\psi \approx 0.3°$. Simulation by Elegant[15] shows that the CSR effect is essentially zero.

ACKNOWLEDGMENTS

The author thanks Drs. S. Krinsky, L.H. Yu, of BNL, and Drs. Z. Huang, T.O. Raubenheimer, J. Welch of SLAC for discussions.

REFERENCES

[1] L.H. Yu, Phys. Rev. A **44**, 5178 (1991); L.H. Yu, *et al.*, Sciences **289**, 932 (2000).

[2] J. Wu, L.H. Yu, Nucl. Instr. Meth. A **475**, 104 (2001); L.H. Yu, Proc. of IFCA, Argonne, (1999).

[3] G. Dattoli, *et al.*, J. Appl. Phys. **86**, 5331 (1999); S.G. Biedron, *et al.*, Nucl. Instr. Meth. A **475**, 401 (2001).

[4] W.B. Colson, IEEE J. Quant. Elect. QE-**17**, 1417 (1981); J.B. Murphy, *et al.* Opt. Com. **53**, 197 (1985).

[5] Z. Huang, K.J. Kim, Phys. Rev. E **62**, 7295 (2000).

[6] T.M. Tran, J.S. Wurtele, Comput. Phys. Commun. **54**, 263 (1989).

[7] W. Fawley, *et al.*, Bull. Am. Phys. Soc. **38**, 1327 (1993); H.P. Freund, Phys. Rev. E **52**, 5401 (1995); E.L. Saldin, *et al.*, Nucl. Instr. Meth. A **429**, 233 (1999).

[8] L.H. Yu, Phys. Rev. E **58**, 4991 (1998); V. Kumar, *et al.*, *ibid.*, **65**, 016503 (2001).

[9] S.G. Biedron, *et al.*, Nucl. Instr. Meth. A **475**, 118 (2001).

[10] A. Doyuran, *et al.*, Phys. Rev. Lett. **86**, 5902 (2001).

[11] M.J. Schmitt, C.J. Elliott, Phys. Rev. A **41**, 3853 (1990).

[12] I. Boscolo, V. Stagno, Nucl. Instr. Meth. A **188**, 483 (1982).

[13] J. Wu, Ph.D. Dissertation, SUNY-Stony Brook (2002); L.H. Yu, J. Wu, Nucl. Instr. Meth. A **483**, 493 (2002).

[14] E.L. Saldin, *et al.*, Opt. Com. **202**, 169 (2002).

[15] M. Borland, Phys. Rev. ST-AB, **4**, 070701 (2001).